

# Diffusion histogram as a marker of fiber crossing within a voxel

B. Wilkins<sup>1</sup>, and M. Singh<sup>2</sup>

<sup>1</sup>Biomedical Engineering, University of Southern California, Los Angeles, California, United States, <sup>2</sup>Radiology and Biomedical Engineering, University of Southern California, Los Angeles, California, United States

**Introduction:** The histogram of the normalized diffusion signal conveys unique statistical information related to the microstructure of the tissue, including the presence of one or more fibers. The objective of this work was to conduct simulation and experimental studies of how the histogram is related to the presence of fibers and the angles between them.

**Method:** The histogram of the normalized diffusion signal is obtained independently for experimental data and simulation results. Experimental case: Whole-brain single shot EPI DTI data were acquired from 4 healthy subjects on a GE Signa HDxt 3.0T scanner (TR=16.6s, FOV=26cm x 26cm, acquisition matrix=128x128, 65 contiguous 2mm thick slices, 55 gradient directions with  $b=1000s/mm^2$ , one  $b=0s/mm^2$  acquisition, and NEX=1) with a total acquisition time of 15min 46sec. Applying the diffusion tensor model permits calculation of Fractional Anisotropy (FA) for each voxel. Voxels with  $FA > 0.8$  are identified and assumed to contain single fiber bundles. The normalized diffusion signal is calculated for all identified voxels and the results are pooled; a histogram is then obtained. The diffusion signal for crossing fibers is *derived* from experimental data by an equal weighted combination of the measured signals from pairs of voxels identified above, with principal eigenvectors separated by a given angle. Simulation case: Assuming a Gaussian model of diffusion, the normalized MR diffusion signal can be expressed analytically as  $S(\bar{g}, b)/S_0 = e^{-b\bar{g}^T D \bar{g}}$  where  $\bar{g}$  is the unit vector  $\bar{q}/|\bar{q}|$ ,  $b$  is given by  $\tau|\bar{q}|^2$ , and  $D$  is the three-dimensional diffusion tensor. The diffusion gradients and  $b$ -value were chosen to reflect the experimental conditions. The eigenvalues for  $D$  were the average values from voxels identified in the experimental data ( $\lambda_1=1.8 \times 10^{-3} mm^2/s$ ,  $\lambda_2=0.29 \times 10^{-3} mm^2/s$ ,  $\lambda_3=0.19 \times 10^{-3} mm^2/s$ ). To simulate crossing fiber bundles the multi-tensor model was used assuming equal weighting of the contributing fibers and no diffusion between compartments (fibers).

Figure 1 identifies the Corpus Callosum (CC) as the dominant location of voxels with  $FA > 0.8$ ; the CC is known to consist of highly aligned fiber bundles. The normalized diffusion signals from all such voxels (total ~160k data points) were pooled from the four subjects, leading to the histogram of Figure 2. For comparison, simulation of the normalized diffusion signal from 1000 randomly oriented single fibers is shown in Figure 3.

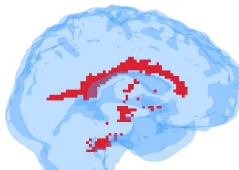


Figure 1 – Location of voxels with  $FA > 0.8$ ; one subject.

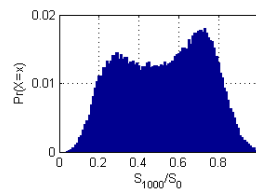


Figure 2 – Histogram of  $S/S_0$  for a single fiber; experimental data.

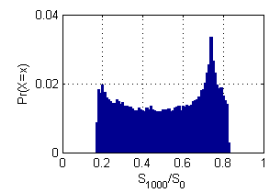


Figure 3 – Histogram of  $S/S_0$  for single fiber; simulation data.

**Results:** Figure 4 illustrates the variation in the histogram for the case of two fibers per voxel, where the inter-fiber angle ranges from 0 to 90°. The experimentally derived data represents pooling of a large number of voxels wherein individual fibers may be oriented differently but the inter-fiber angles are matched (within  $\pm 0.5^\circ$ ). As such, these histograms are equivalent to gradient sampling over a very large number of directions. For comparison, histograms of simulation data corresponding to the diffusion signal of a *single* voxel is included in Figure 4, for 55 and 512 diffusion gradient schemes. As a quantitative measure of the non-Gaussianity of the histogram, the normalized Kurtosis ( $kurt(N(0,1)) = 0$ ) is included in Figure 4 for the experimentally derived data.

Figure 4	Angle between two crossing fibers							
	$0 \pm 0.5^\circ$	$10 \pm 0.5^\circ$	$20 \pm 0.5^\circ$	$40 \pm 0.5^\circ$	$50 \pm 0.5^\circ$	$70 \pm 0.5^\circ$	$80 \pm 0.5^\circ$	$90 \pm 0.5^\circ$
Exp'ment. Data								
Kurtosis	-1.2469	-1.2330	-1.2029	-0.9825	-0.7788	-0.3055	-0.1631	-0.1204
Simulation Data (512 grad.)								
Simulation Data (55 grad.)								

Figure 4 – Histogram of normalized diffusion signal ( $S/S_0$ ) for two crossing fibers; experimentally derived and simulation results presented for comparison.

**Discussion:** The histogram of Figure 2 reveals a unique distribution of  $S/S_0$  for a single fiber. Figure 3 is the corresponding simulation result, which is in agreement except for the sharp tapering of the distribution tails. This is thought to be associated with use of the analytical expression for the simulated normalized diffusion signal, which does not account for effects caused by tissue architecture, and is noise free. The experimental histograms of Figure 4 reveal a progressively Gaussian distribution of  $S/S_0$  as the inter-fiber angle increases. With the addition of a second fiber, and with increasing inter-fiber angle, the increased restriction in diffusion means less diffusion directions experience large signal loss (low  $S$ ), and thus the low end of the histogram moves to progressively higher  $S/S_0$ .

While the results presented are for two fibers per voxel, the method could be extended to three or more fibers. The well defined shape of Figure 2 suggests that specific changes to the distribution could be mapped to pathological changes in tissue. Furthermore, the histogram results of Figure 4 indicate the possibility of using the histogram as a unique indicator of the number of fibers per voxel, and the inter-fiber angle.

**References:** [1] Basser, P., *et al*, J. Magn. Reson. B (103), 247-254. [2] Behrens, T.E.J., *et al*, NeuroImage 34 (1), 144-155.